ELSEVIER

Journal of Photochemistry and Photobiology A: Chemistry 149 (2002) 169–174

Journal of Photochemistry and Photobiology A:Chemistry

www.elsevier.com/locate/jphotochem

Photocatalytic degradation of cationic azo dye by TiO_2/bentonite nanocomposite

Zhenshi Sun [a,*], Yingxu Chen [a], Qiang Ke [a], Ye Yang [a], Jun Yuan [b]

[a] *Department of Environmental Engineering, Zhejiang University, Hangzhou 310029, PR China*
[b] *State Key Laboratory of Si Material Science, Zhejiang University, Hangzhou 310029, PR China*

Received 10 July 2001; received in revised form 19 November 2001; accepted 29 November 2001

Abstract

Titanium dioxide/bentonite clay nanocomposite prepared by acid-catalyzed sol–gel method was used as photocatalyst in the reaction of cationic azo dye decomposition in water. The incorporation of TiO_2 was confirmed by powder X-ray diffraction (XRD) and X-ray photoelectron spectrometer (XPS). The photocatalytic activity of those nanocomposite photocatalysts was much higher than that of the pure titanium dioxides. The nanocomposite created a kinetic synergy effect in Cationic Red GTL (GTL) disappearance with an increase of the rate constant by a factor of 2.57 for neat TiO_2 (P-25). The photo-activities were greatly dependent on the solution pH, and it was more effective for GTL to be degraded under alkaline condition. That was likely to contribute for the acid–base equilibria on the surface of the nanocomposite. Results also indicated that the proper addition of hydrogen peroxide could improve the decolorization rate, but the excess hydrogen peroxide could quench the formation of $^{\bullet}OH$.

Keywords: Nanocomposite; Bentonite clay; Cationic Red GTL; Photocatalytic degradation; Titanium dioxide

1. Introduction

In recent years, the arising ecological problems connected with the presence of potentially carcinogenic compounds have been widely observed. In addition, these dangerous compounds are often nonbiodegradable or toxic to microorganisms and have very long degradation time in the environment [1–5]. Wastewaters produced from textile and other dyestuff industrial processes contain large quantities of azo dyes constituting a significant portion and having the least desirable consequences in terms of surrounding ecosystems. They are also resistant to aerobic degradation and under anaerobic conditions they can be reduced to potentially carcinogenic aromatic amines [6,7].

Photocatalytic reactions of semiconductors such as decomposition of waste pollutants have received special attention in the decomposition of hazardous organic compounds because of their complete mineralization ability and possible application to pollution control using solar energy [8–13]. Typically, the process is initiated by band-to-band excitation of semiconductor particles by radiation to generate $^{\bullet}OH$ radicals derived from valence band hole oxidation of terminal OH^- groups and water of hydration on the particle surface. These extremely reactive radicals have been postulated as the dominant oxidizing agents, which appear to control the overall kinetics of the oxidative process [14–17]. It is to be expected that the photoactivity of semiconductor increases with the decrease of particle size, especially when the crystallite dimension of a semiconductor particle falls below a critical radius of approximately 10 nm since, in such a system, the charge carriers appear to behave quantum mechanically. Holes and electrons can be effectively captured by the electrolyte in the solution, which may result in increased rate constant of charge transfer. Thus, the use of sizequantized semiconductor particles is expected to increase the photo-efficiencies [10,18,19].

Recently, semiconductor/lamellar nanocomposite have been receiving much interest [20–24]. Bentonite clay, which is cheap and widely used in wastewater treatment as adsorbent, is also a lamellar crude mineral. The layer structure of bentonite consists of two silica tetrahedral sheets fused to one alumina octahedral sheet. Shackong of the layers of ca. 1 nm in thickness by weak dipolar force leads to interlayer galleries. The galleries are normally occupied by such cations as Na^+, Ca^{2+} and Mg^{2+}. TiO_2/bentonite composite catalyst can be obtained by cation exchange reaction with polynuclear cationic species. During in situ intercalation

* Corresponding author. Tel.: +86-571-86971157; fax: +86-571-86971411.
E-mail address: sunzs@zju.edu.cn (Z. Sun).

1010-6030/02/$ – see front matter
PII: S1010-6030(01)00649-9

process, some nanoscale particles are dispersed in the interlayer. Miyoshi et al. [21] and Sterte [25] had reported the incorporation of extremely small particles of Fe_2O_3, and TiO_2, <1 nm in thickness, into the interlayer of montmorillomite clay. But their studies did not focus on the evaluation of activities in photocatalytic degradation contaminants of the retained semiconductor particles.

In this paper, we have developed a new method for preparation of active TiO_2/bentonite nanoscale composite photocatalyst and reported the results for the photocatalytic degradation of azo dyes using this active composite photocatalyst in suspension system. Physical characterization of this material was reported employing powder X-ray diffraction (XRD) and X-ray photoelectron spectrometer (XPS). The effects of the solution pH on the rate of decolorization were examined because of the possible presence in natural water systems. The effect of the addition of H_2O_2 was also discussed for enhancement of elimination of azo dyes.

2. Experimental

2.1. Materials

Bentonite clay was obtained from Liaoning, China. Impurity quartz was removed by fractionation using conventional sedimentation techniques. The cation exchange capacity of the bentonite was determined to be 115 mequiv./100 g. Cationic Red GTL (GTL), was of laser grade quality (Hangzhou Jinjiang Chemical) and was used directly without further purification. TiO_2 (Shanghai, average particle size as measured by SEM about 0.95 μm, mainly of anatase form confirmed by XRD), was of chemical purity. TiO_2 (Degussa P-25, 30 nm mean particle size, mainly anatase (ca. 70%)) was obtained from the Degussa (Germany). Tetrabutyl titanate and all other chemicals were of analytical reagent grade quality and were employed without further purification. The structure of the GTL molecule was illustrated below.

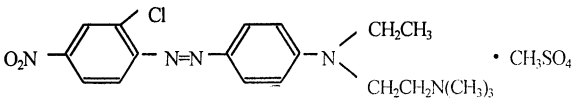

2.2. Preparation of TiO_2/bentonite nanocomposite

The TiO_2 sol was synthesized by the method called acid-catalyzed sol–gel process. The reactant composition was 20 ml 1 M HNO_3, 8.5 ml tetrabutyl titanate and 10 ml ethanol.

Firstly, $Ti(OC_4H_9)_4$ was added to ethanol, stirring at the same time, followed by agitation for 0.5 h to give a flaxen transparent solution. Then, the solution was added dropwise to 1 M HNO_3 aqueous solution under vigorous stirring at the same time, followed by agitation for 1.5 h to give a transparent TiO_2 sol. The pH of the colloidal solution was adjusted to 1.5 with addition of 1 M NaOH.

The 2 g bentonite clay saturated with water for half an hour was mixed with a certain amount of TiO_2 sol, with stirring for 1 h, then followed by washing–centrifugation procedure to make the supernatant nearly neutral. The cations such as Na^+, Ca^{2+} and Mg^{2+} were exchanged with polynuclear cationic species $((TiO)_8(OH)_{12})^{4+}$. The mixture was dried for almost 40 h at 50 °C, calcined at 500 °C for 2.5 h, then those polynuclear cationic species in the galleries went further hydrolyzing and dehydration to TiO_2. Finally, the heated products were ground into fine powder. All the samples were stored in the dark to avoid preactivation by room light.

2.3. Photocatalytic decomposition of azo dye

The experiments were carried out in a photocatalytic oxidation reactor as that shown in Sabate's experiments [26]. In the center of the cylindrical reactor, two 6 W (E_{max} = 365 nm) UV lamps were used as the light resource. The relative photocatalytic activities of various catalysts were evaluated by measuring the loss of dye GTL in aqueous medium as a representative reaction. Prior to commencing illumination, a suspension containing 1.35 g of catalyst and 450 ml of GTL was stirred continuously on the dark for 12 h before irradiation. The concentration of substrate in bulk solution concentration at this point was used as the initial value for the further kinetic treatment of the photodegradation processes. It was cooled by water circulation to 20 °C during the experiments. All irradiations were carried out under constant stirring. Distilled water was used throughout the work. The pH of the solution was adjusted with either dilute HNO_3 or NaOH.

At given intervals of illumination, a sample of the catalysts particulate was collected, centrifuged, and then filtered through a Millipore filter (pore size 0.22 μm). The filtrates were analyzed by UV–Vis spectroscopy using a UV1206 spectrophotometer. The determination wavelength is 490.5 nm for GTL, which is the maximum absorption wavelength. The determined absorption was converted to concentration through the standard curve method of dyes ($r = 0.9998$).

2.4. Characterization analysis

The phase composition of photocatalyst was studied by the powder XRD technique. The patterns were recorded on a Rigaku X-ray diffractometer using Cu Kα radiation. Diffraction patterns were taken over the 2θ range 3–70°. XPS were recorded with Escalab MKII XPS with Al Kα radiation operated at 15 kV and 300 W. Calibration of the spectra was done at the C(1s) peak surface contamination at 285.0 eV.

3. Results and discussion

3.1. Characterizations of photocatalyst

Fig. 1 showed the X-ray powder patterns of bentonite clay, the 50 °C treated sample (TiO_2/bentonite), and the 500 °C treated sample (TiO_2/bentonite). The 2θ angle of the (0 0 1) reflection corresponding to the basal spacing of the clays were 5.88° for the bentonite clay, 5.60° for the 50 °C treated sample, and 9.06° for the 500 °C treated sample. These corresponded to d(0 0 1) basal spacings of 1.50, 1.58 and 0.98 nm for the bentonite clay, 50 °C treated sample, and 500 °C treated sample, respectively. This result demonstrated the insertion of polynuclear cationic species by cation exchange reaction with the cations such as Na^+, Ca^{2+} and Mg^{2+} in the galleries of bentonite clay, and the formation of nanosize particle in the galleries of the bentonite clay through the iron exchange reactions [25,27].

The determination results of XPS analysis suggested that no Ca^{2+} or Na^+ but Ti^{4+} was found in the TiO_2/bentonite, in comparison with the initial purified bentonite clay. The binding energies of Ti(2p) of TiO_2/bentonite were basically equal to that of pure TiO_2. It also proved the complete cation exchange reaction between the inorganic cations in the gallery of bentonite clay and the titanium polynuclear cation species.

3.2. Photocatalytic kinetics of azo dyes by different photocatalysts

The absorption spectra of an aqueous solution of GTL recorded following the subsequent illumination of the aqueous TiO_2/bentonite nanocomposite dispersion during a 4 h period are shown in Fig. 2. Generally, azo dyes are characterized by nitrogen to nitrogen double bond (–N=N–) [28]. The colors of azo dyes are determined by azo bonds and their associated chromophores and auxochromes. The intensity of the 490.5 nm absorption peaks corresponding to the red dye decreased rapidly following photolysis. Concomitantly, no new adsorption peaks appeared. This confirmed the photodegradation of GTL, i.e., the breakup of the chromophore responsible for the characteristic color of the azo dyes, rather than its discoloration or bleaching, as deethylation results in a blue-shift of the absorption bands seen in the 400–600 nm region. It also indicated that the –N=N– bond of the dyes in this study were the most active sites for oxidative attack. Similar results were also found by Zhan and Tian [28] for the photocatalytic degradation of H/K acid azo dyes. The color of the dispersion disappeared at the end of the irradiation period, as evidenced by the near total loss of absorption in this wavelength range, although the presence of some aromatic intermediate species was not preclude (note, e.g., the spectral features at wavelengths below 320 nm).

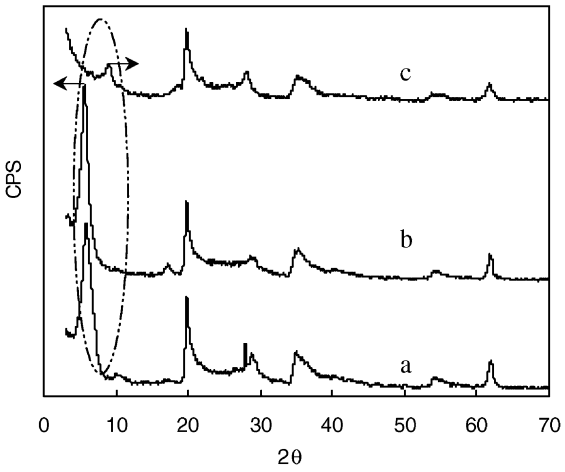

Fig. 1. XRD patterns of: (a) bentonite clay; (b) TiO_2/bentonite treated at 50 °C; (c) TiO_2/bentonite treated at 500 °C (TiO_2/bentonite nanocomposite).

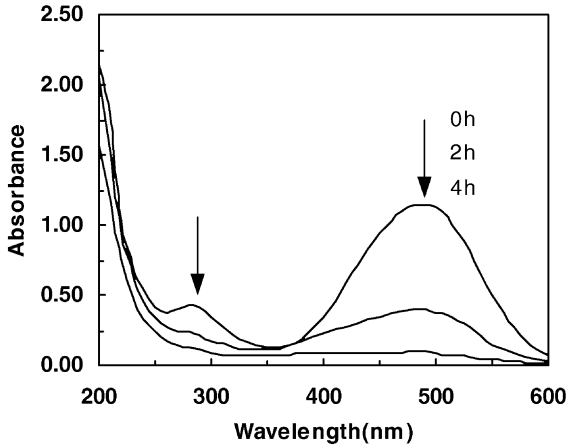

Fig. 2. UV–Vis spectral changes of GTL in aqueous TiO_2/bentonite nanocomposite dispersions as a function of irradiation time.

Control experiments established that GTL did not degrade in TiO_2/bentonite nanocomposite suspensions in the dark. When illuminated with UV only here was less than 5% degradation for GTL. Therefore, we inferred from this that both UV light and TiO_2/bentonite nanocomposite particles were indispensable to the photocatalytic oxidative degradation of GTL.

To compare the catalytic activity of plain TiO_2 and TiO_2/bentonite nanocomposite, 3 mg/l TiO_2 (Shanghai), P-25 and TiO_2/bentonite nanocomposite were used in the 140 mg/l solution, respectively. All the results are presented in Fig. 3. The irradiated TiO_2/bentonite nanocomposite eliminated 90.1% GTL from the solution within 4 h. In contrast, the pure titanium dioxide, P-25, only gives 58.7% disappearance of GTL.

In general, most dependencies of the photocatalytic reaction rates on the concentration of organic pollutants have been described well by the Langmuir–Hinshelwood kinetic

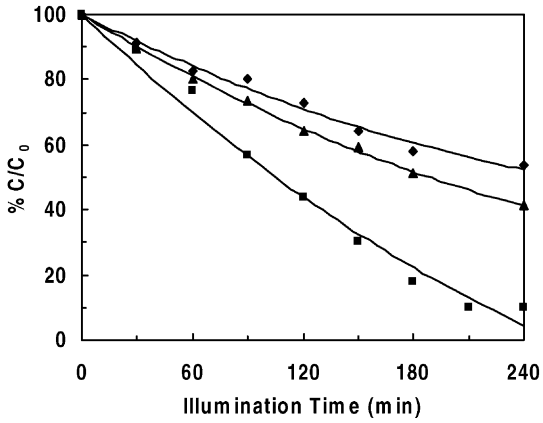

Fig. 3. Decolorization of cation red GTL in the presence of illuminated pure TiO_2 (Shanghai) (◆), P-25 (▲) and TiO_2/bentonite nanocomposite (■).

model, i.e. [8,29]

$$r = \frac{dC}{dt} = \frac{kKC}{1 + KC} \quad (1)$$

The above equation can be simplified to a pseudo-first-order equation

$$\ln\left(\frac{C_0}{C}\right) = kKt = k't \quad (2)$$

where r is the oxidation rate of the reactant (mg/l·min), C_0 the initial concentration of the reactant (mg/l), C the concentration of the reactant at time t (mg/l), t the illumination time, k the reaction rate constant (min^{-1}), and K the adsorption coefficient of the reactant onto the semiconductor particles (l/mg).

The kinetic curves in Fig. 3 were of the apparent first order as confirmed by the linear transform $\ln(C_0/C) = kt + b$, giving apparent rate constants respectively, equal to the following:

- TiO_2 (Shanghai): $k_{app} = 0.0026\,min^{-1}$,
- P-25: $k_{app} = 0.0037\,min^{-1}$,
- TiO_2/bentonite nanocomposite: $k_{app} = 0.0095\,min^{-1}$.

Then, it could be seen that the photocatalytic activity of the TiO_2/bentonite nanocomposite system determined from the apparent rate constant was much higher than that of neat TiO_2. The nanocomposite created a kinetic synergy effect in GTL disappearance with an increase of the rate constant by a factor of 4.13 to pure TiO_2 (Shanghai) and 2.57 to P-25. It indicated that the electrons and holes photoinduced from intercalated TiO_2 could be much more effectively separated in the photocatalytic degradation of GTL than the unsupported TiO_2. The depression of the recombination of electrons and holes might be due to the difference between the nanoscale titanium dioxides incorporated in the interlayer and those of unsupported ones. Wu et al. [30] found that the photocatalytic hydrogen production activities of TiO_2/$HNbWO_6$ and Fe_2O_3/$HNbWO_6$ nanocomposites were superior to those of unsupported TiO_2 and Fe_2O_3. Fujishiro et al. [31] also found that the photocatalytic activities of semiconducting layer compounds, such as $H_4Nb_6O_{17}$, incorporated of semiconductors in the interlayers were much more efficient than those of unsupported ones. Recently, it had been reported that there were some evidences about the charge transfer between the guest and host. In study of the mechanisms for the high photoactivity of CdS pillared montmorillomite by Fujishiro et al. and $Cd_{0.8}Zn_{0.2}S$ pillared $H_{1-x}Ca_{2-x}La_xNb_3O_{10}$ by Fukugami et al. by the way of measuring the fluorescence intensity and life time, both the two groups found that the guest-to-host electron transfer seemed to play an important role to improve the photocatalytic activity [23,31]. Therefore, the high photoactivity of TiO_2/bentonite nanocomposite had been effected by the synthetic functions of several factors. Further study was necessary to clear the mechanism for the high photocatalytic activity of TiO_2/bentonite nanocomposite.

Moreover, the nanocomposite catalysts had an advantage over the pure titanium dioxide. They had good sedimentation ability and could decant in a few minutes. Indeed, some sedimentation experiments carried out in the same experimental condition showed that TiO_2/bentonite nanocomposite decanted from the suspension in about 10 min, while the pure TiO_2 did not decant after 12 h.

3.3. Effect of initial pH

The influence of the pH on the decolorization extent for GTL was shown in Fig. 4. The degradation curves of GTL were presented as time-dependent normalized dye concentration in the solution. The results showed that there was a strong dependence of the pH of the solution on the heterogeneous photo-process. Alkaline pH values had been found to be favorable for the photocatalytic degradation of pollutant molecules in their cationic form. It is known that metal oxide particles suspended in water behave similar to diprotic acids. For TiO_2, hydroxyl groups undergo the following

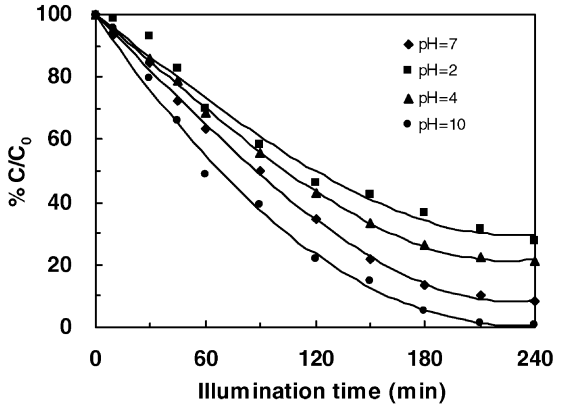

Fig. 4. Effect of initial pH on the photodegradation of GTL. Initial concentration of GTL was 140 mg/l.

two acid–base equilibria:

$$\geq TiOH_2^+ \rightleftharpoons \geq TiOH + H^+, \quad pK_{a1} \tag{3}$$

$$\geq TiOH \rightleftharpoons \geq TiO^- + H^+, \quad pK_{a2} \tag{4}$$

for Degussa P-25, $pK_{a1} = 4.5$ and $pK_{a2} = 8.0$, which yield a pH of zero point charge equal to $pH_{zpc} = 6.25$. Generally, for charged substrates, a significant dependency of the photocatalytic degradation efficiency upon pH value had been observed, since the overall surface charge and hence the adsorptive properties of TiO_2 particles depend strongly on solution pH [7,32].

The bentonite clay usually has Ca^{2+}, Na^+ and Mg^{2+} in its interlayers to compensate negative charges of silicate layers. In the preparation of TiO_2/bentonite, the Ca^{2+}, Na^+ and Mg^{2+} ions were replaced by positively charged polynuclear cation species, which were then decomposed to give titanium dioxide incorporated bentonite clay. Since the resulting titanium dioxide must be electrically neutral, adsorption of protons must occur on the oxide surfaces to keep electrical neutrality of the clay. Therefore, for TiO_2/bentonite nanocomposite, there are probably acid–base equilibria on the surface of the nanocomposite, too (Eqs. (5) and (6)). Mishra and Parida [33] had found the total acidity and the strong acid sites of chromia-pillared montmorillomite. Thus, it is reasonable to expect that adsorption on nanocomposite will depend on the electrical charge of the dye and the photocatalyst surface. The cationic azo dye molecular was hydrolyzed into organic cations and inorganic anions in solution. At alkaline solution, attractive forces between the organic cation and the photocatalyst surface will favor adsorption. On the other hand, at low pH, the photocatalyst surface is positive charged and repulsive forces will lead to decreased adsorption:

$$\geq MOH_2^+ \rightleftharpoons \geq MOH + H^+ \tag{5}$$

$$\geq MOH \rightleftharpoons > M\text{–}O^- + H^+ \tag{6}$$

3.4. Effect of added H_2O_2

Limitation to the rate of photocatalytic degradation had been attributed to the recombination of photogenerated hole–electron pairs [34,35]. The addition of inorganic oxidant may play important roles in accelerating the degradation rate of azo dyes. In this work reported here, experiments were conducted to examine the effect of H_2O_2 on the UV/(TiO_2/bentonite) nanocomposite system. The degradation rate of GTL increased by the addition at the beginning of the reaction solution of 4, 6, and 12 mmol/l H_2O_2 as shown from the results in Fig. 5. It seemed that the photocatalytic degradation rates of GTL could also be increased efficiently with the addition of H_2O_2. However, experiments with initial H_2O_2 concentration of 12 mmol/l, showed that the rates of the photocatalytic reaction decreased.

In a study of the role of H_2O_2 in the photocatalytic degradation of 1,2-dimethoxybenzene (1,2-DMB) using catalase and superoxide dismutase, Amalric et al. [36] also found that the addition of H_2O_2 to the UV/TiO_2 system had either favorable or unfavorable effect which depends on the ratio of [H_2O_2]/[1,2-DMB]. Similar results were also obtained by Pacheco et al. for the photocatalytic degradation of trichloroethylene and salicylic acid, and by Cornish et al. for the photodegradation of microcystin-LR [37,38]. The higher reaction rates after the addition of peroxide were attributed to the increase in the concentration of hydroxyl radical. At low concentration of hydrogen peroxide, H_2O_2 could increase the rate of hydroxyl radical formation though three ways. Firstly, the hydroxyl radicals would be available for attack on the –N=N– bond. Firstly, it could act as an alternative electron acceptor to oxygen (Eq. (7)), which might restrain the bulk-composite of the photo-excitated electrons and holes. This should consequently increase the rate of the photocatalytic process. Secondly, the reduction of H_2O_2 at the conductance band would also produce hydroxyl radicals. Even if H_2O_2 was not reduced at the conductance band it could accept an electron from superoxide again producing hydroxyl radicals (Eq. (8)). Thirdly, the self-decomposition by illumination would also produce hydroxyl radicals (Eq. (9)):

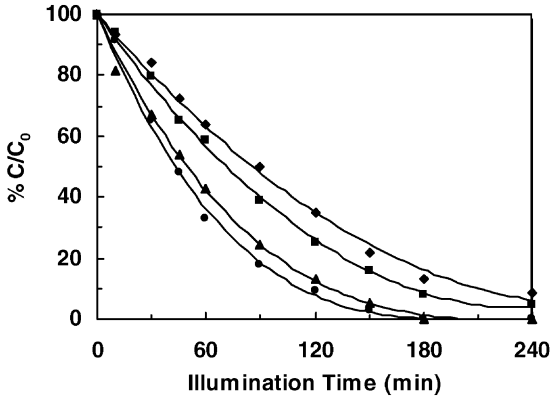

Fig. 5. Effect of H_2O_2 on the photodegradation of GTL. Initial concentration of GTL was 140 mg/l: (◆) no H_2O_2, (▲) H_2O_2, 4 mg/l, (●) H_2O_2, 6 mg/l and (■) H_2O_2, 12 mmol/l.

$$e_{CB}^- + H_2O_2 \rightarrow OH^- + {}^\bullet OH \tag{7}$$

$${}^\bullet O_2^- + H_2O_2 \rightarrow OH^- + {}^\bullet OH + O_2 \tag{8}$$

$$H_2O_2 + h\nu \rightarrow 2{}^\bullet OH \tag{9}$$

At high concentrations, the hydrogen peroxide, sorbed on the photocatalyst surface could effectively scavenge not only the photocatalyst surface-formed $^\bullet$OH radicals (Eqs. (10) and (11)) but also the photo-generated holes (h_{CB}^+) (Eq. (12)) and thus inhibit the major pathway for heterogeneous generation of $^\bullet$OH radicals:

$${}^\bullet OH + H_2O_2 \rightarrow H_2O + {}^\bullet HO_2 \tag{10}$$

$${}^\bullet HO_2 + {}^\bullet OH \rightarrow H_2O + O_2 \tag{11}$$

$$h_{CB}^+ + H_2O_2 \rightarrow H^+ + {}^\bullet HO_2 \tag{12}$$

Therefore, the proper addition of hydrogen peroxide could accelerate the degradation rate of cationic azo dyes. However, in order to keep the efficiency of the added hydrogen peroxide, it was necessary to choose the proper dose of hydrogen peroxide according to the kinds and the concentrations of pollutants.

4. Conclusions

The results presented in this paper indicated that TiO_2 could be intercalated into the interlayer of bentonite clay by the method of acid-catalyzed sol–gel process, and the photodegradation of azo dyes using TiO_2/bentonite nanocomposite as a catalyst should be considered as a promising alternative to wastewater purification. The photocatalytic activity of the TiO_2/bentonite nanocomposite system determined from the apparent rate constant was much higher than that of neat TiO_2. The nanocomposite created a kinetic synergy effect in GTL disappearance with an increase of the rate constant by a factor of 4.13 for neat TiO_2 (Shanghai) and 2.57 to P-25. The nanocomposite photocatalyst forms nanoscale titanium dioxides in the galleries of the bentonite, which were probably responsible for the higher photoactivity. Moreover, the nanocomposite catalysts had good sedimentation ability. They could decant in a few minutes. The results of this work may establish a new preparation method of active nanocomposite photocatalyst.

The photocatalytic activities of the nanocomposite were greatly dependent on the solution pH, and alkaline pH values have been found to be favorable for the photocatalytic degradation of pollutant molecules in their cationic form. That was likely to contribute for the acid–base equilibria on the surface of the nanocomposite. The proper addition of hydrogen peroxide could improve the decolorization rate. However, excess H_2O_2 would quench the formation of $^{\bullet}OH$.

Acknowledgements

The authors are grateful to Professor Guanglie Lu for the XRD measurement.

References

[1] Y. Ono, S. Mohri, I. Somiy, Y. Oda, Environ. Mut. Res. 17 (1995) 179–186.
[2] F. Wania, J. Axelaman, D. Broman, Environ. Pollut. 102 (1998) 3–23.
[3] F. Wania, D. Mackay, Environ. Pollut. 100 (1999) 223–240.
[4] R. Panades, A. Ibarz, S. Esplugas, Wat. Res. 34 (2000) 2951–2954.
[5] O. Yoshiro, S. Isao, O. Yoshimitsu, Wat. Res. 34 (2000) 890–894.
[6] R. Nilsson, R. Nordlinder, U. Wass, Br. J. Ind. Med. 50 (1993) 65–70.
[7] W.Z. Tang, H. An, Chemosphere 31 (1995) 4157–4170.
[8] R.W. Matthews, J. Catal. 111 (1988) 264–272.
[9] D. Mas, P. Pichat, C. Guillard, Res. Chem. Intermed. 23 (1997) 275–290.
[10] H. Osora, W. Li, L. Otero, M.A. Fox, J. Photochem. Photobiol. B 43 (1998) 232–238.
[11] K. Wang, Y. Hisieh, C. Wu, M. Chou, C. Chang, Appl. Catal. B 21 (1999) 1–8.
[12] J. Grzechulska, M. Hamerski, A.W. Morawski, Wat. Res. 34 (2000) 1638–1644.
[13] I. Konatantinou, T.M. Sakellarides, V. Sakkas, T.A. Albanis, Environ. Sci. Technol. 35 (2001) 398–405.
[14] C.D. Jaeger, A.J. Bard, J. Phys. Chem. 83 (1979) 3146–3152.
[15] C.S. Turchi, D.F. Ollis, J. Catal. 122 (1990) 178–192.
[16] R.W. Matthews, R.S. McEvoy, J. Photochem. Photobiol. A 64 (1992) 231–246.
[17] K. Ishibashi, A. Fujishima, T. Watanabe, K. Hashimoto, J. Photochem. Photobiol. A 134 (2000) 139–142.
[18] M.R. Hoffmann, S.T. Martin, W. Choi, D.W. Bahnemann, Chem. Rev. 95 (1995) 69–96.
[19] K. Kato, Y. Torii, H. Taoda, T. Kato, Y. Butsugan, K. Niihara, J. Mater. Sci. Lett. 15 (1996) 913–915.
[20] H. Yoneyama, S. Haga, J. Phys. Chem. 93 (1989) 4833–4837.
[21] H. Miyoshi, H. Mori, H. Yoneyama, Langmuir 7 (1991) 503–507.
[22] J. Wu, S. Uchida, Y. Fujishiro, S. Yin, T. Sato, Int. J. Inorg. Mater. 1 (1999) 253–258.
[23] Y. Fukugami, T. Sato, J. Alloys Compounds 312 (2000) 111–118.
[24] M. Yanagisawa, T. Sato, Int. J. Inorg. Mater. 3 (2001) 157–160.
[25] J. Sterte, Clays Clay Miner. 34 (1986) 658–664.
[26] J. Sabate, M.A. Anderson, H. Kikkawa, M. Edwards, C.G. Hill, J. Catal. 134 (1991) 36–46.
[27] G. Chen, Y. Ma, Z. Qi, Scripta Mater. 44 (2001) 125–128.
[28] H. Zhan, H. Tian, Dyes and Pigments 37 (1998) 231–239.
[29] D.F. Ollis, Environ. Sci. Technol. 19 (1985) 480–484.
[30] J. Wu, S. Uchida, Y. Fujishiro, S. Yin, T. Sato, J. Photochem. Photobiol. A 128 (1999) 129–133.
[31] Y. Fujishiro, S. Uchida, T. Sato, Int. J. Inorg. Mater. 1 (1999) 67–72.
[32] K. Wang, Y. Hisieh, C. Wu, C. Chang, Chemosphere 40 (2000) 389–394.
[33] T. Mishra, K. Parida, Appl. Catal. A 166 (1998) 123–133.
[34] G.K.-C. Low, S.R. McEvoy, R.W. Matthews, Environ. Sci. Technol. 25 (1991) 460–467.
[35] D.D. Dionysiou, M.T. Suidan, E. Bekou, I. Baudin, J. Laine, Appl. Catal. B 26 (2000) 153–171.
[36] L. Amalric, C. Guillard, P. Pichat, Res. Chem. Intermed. 20 (1994) 579–594.
[37] J.E. Pacheco, G.E. Tyne, Solar engineering 1990, in: Proceedings of the 1990 ASME International Solar Energy Conference, Miami, FL, April 1–4, 1990, pp. 163–166.
[38] B.J.P.A. Cornish, L.A. Lawton, P.K.J. Robertson, Appl. Catal. B 25 (2000) 59–67.